Letters

General Analysis of Fibonacci Charge Pump SSL Output Characteristics With Parasitic Capacitances

Alexander Oliva, *Member, IEEE*, and Jeffrey H. Lang, *Fellow, IEEE*

***Abstract*—A closed-form analytic formula for the output characteristics of a Fibonacci charge pump model in the slow-switching limit generalized to any number of switching capacitor stages is derived for the first time. The model incorporates bottom-plate and closed-switch parasitic capacitances. Thus, the derived formula gives insight into the effects of parasitics on the output characteristics and their deviation from the ideal, including the limit of the output resistance and gain as the number of stages grows to infinity. The limits of this generalized formula reduce to previously published results of special cases, and simulations confirm the results. The calculation complexity of the output characteristics using the model is completely independent of the size of the converter, whereas the computational complexity of previous works grows linearly with converter size.**

***Index Terms*—Circuit analysis, dc–dc power conversion, switched capacitor (SC) circuits, voltage multipliers.**

I. Introduction

SWITCHED-CAPACITOR charge pumps are an attractive type of power converter because of their operation without magnetic components, which allows for monolithic implementations and higher power densities than inductor-based converters [1]. In particular, the Fibonacci charge pump (FQP) has the maximum theoretical output voltage in ideal cases [2], [3]. The FQP has also been shown to most effectively minimize capacitor size in discrete designs where the bottom-plate parasitic capacitance factor is less than 1% [4]. As a result, the FQP is of particular interest in many applications.

In order to understand the effects of parasitic capacitances on the FQP, previous methods relied on large matrices to calculate charge pump characteristics. Some previous matrix-based approaches used charge multiplier vectors that grow in length proportionally to N, the number of switching capacitors, to cal-

Manuscript received December 18, 2018; revised January 21, 2019; accepted February 6, 2019. Date of publication February 20, 2019; date of current version June 10, 2019. The work of A. Oliva was supported by a graduate fellowship from Draper Laboratory while executing the work reported herein. *(Corresponding author: Alexander Oliva.)*

A. Oliva was with the Department of Electrical Engineering and Computer Science, Massachusetts Institute of Technology, Cambridge, MA 02139 USA (e-mail:

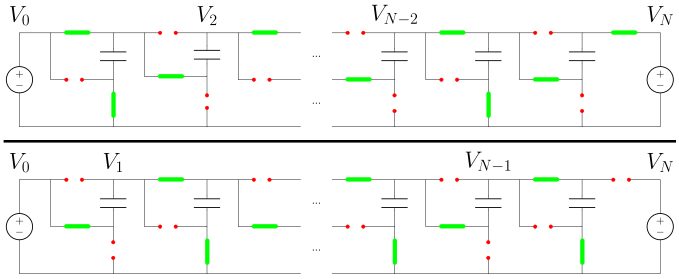

Fig. 1. Two phases of FQP circuit with N switching capacitors. Thick bars and open dots indicate closed and open switches, respectively.

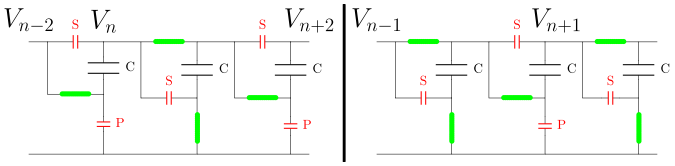

Fig. 2. Illustration of voltage changes across all capacitors at intermediate node V_n by comparing first phase (left) to second phase (right).

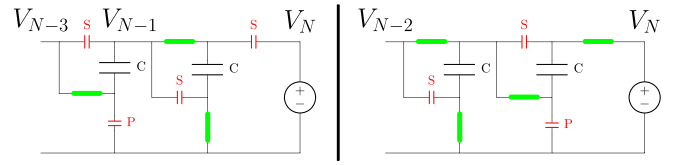

Fig. 3. Illustration of voltage changes across all capacitors at intermediate node V_{N-1} by comparing first phase (left) to second phase (right).

100-V output voltages, including energy harvesting or compact inductor-less low-voltage designs. In these cases, the voltage ratings of the capacitors can all be sized equally for typical capacitors, allowing the same capacitor part to be used for all switching capacitors. In large production volumes, this can dramatically reduce cost. Similarly to capacitor-sizing, by using the same part for all switches, the parasitic open-switch capacitances can be approximately assumed as equal across the circuit in this voltage range. The resulting equations of this letter provide optimization tools with several computational advantages over previous works to maximize the output voltage for a specified load.

B. Derivation of Output Characteristics

Analyzing the charge flow at V_n for $0 < n < N$ leads to a matrix representation of all intermediary voltages in the FQP that exist for $N \geq 2$. Figs. 2 and 3 show both phases of the FQP that affect the current flow into V_n for $0 < n < (N-1)$ and $n = (N-1)$, respectively. Summing the charge flow out of V_n for $0 < n < (N-1)$ and $n = (N-1)$, respectively, results in

$$\begin{aligned} &C[(V_n - V_{n-2}) - (V_{n-1})] + C[(V_n) - (V_{n+1} - V_{n-1})] \\ &- C[(V_{n+2} - V_n) - (V_{n+1})] + S[(V_n - V_{n-2}) - (0)] \\ &+ S[(V_n) - (0)] + S[(V_n - V_{n+2}) - (0)] + P[(V_n) - (0)] \\ &\qquad = 0 \text{ for } 0 < n < (N-1) \end{aligned} \tag{1}$$

and

$$\begin{aligned} &C[(V_{N-1} - V_{N-3}) - (V_{N-2})] + C[(V_{N-1}) - (V_N - V_{N-2})] \\ &+ S[(V_{N-1} - V_{N-3}) - (0)] + S[(V_{N-1}) - (0)] \\ &+ S[(V_{N-1} - V_N) - (0)] = 0 \text{ for } n = (N-1) \end{aligned} \tag{2}$$

which simplifies to

$$\begin{aligned} &-(C+S)V_{n-2} + (3C+3S+P)V_n - (C+S)V_{n+2} = 0 \\ &\qquad \text{for } 0 < n < (N-1) \end{aligned} \tag{3}$$

and

$$\begin{aligned} &-(C+S)V_{N-3} + (2C+3S)V_{N-1} = (C+S)V_N \\ &\qquad \text{for } n = (N-1). \end{aligned} \tag{4}$$

In the case where $n = 1$, the value of V_{n-2} is equal to V_0 as can be seen by comparing Figs. 1 with 2 for $N > 2$ or by comparing Figs. 1 with 3 for $N = 2$. Note that the system when $N = 1$ has no intermediary voltages and is therefore not relevant to (1)–(19). However, for $N \geq 2$, (3) and (4) can be used to represent the intermediary voltages V_1 through V_{N-1} by

$$(C\mathbf{C_m} + S\mathbf{S_m} + P\mathbf{P_m})\,\bar{v} = (C+S)\mathbf{B}\begin{bmatrix} V_0 \\ V_N \end{bmatrix} \tag{5}$$

with $(N-1) \times (N-1)$ matrices

$$\mathbf{C_m}(i,j) = \begin{cases} 3 & \text{if } i = j \neq (N-1) \\ 2 & \text{if } i = j = (N-1) \\ -1 & \text{if } i = j \pm 2 \\ 0 & \text{otherwise} \end{cases} \tag{6}$$

$$\mathbf{S_m}(i,j) = \begin{cases} 3 & \text{if } i = j \\ -1 & \text{if } i = j \pm 2 \\ 0 & \text{otherwise} \end{cases} \tag{7}$$

$$\mathbf{P_m}(i,j) = \begin{cases} 1 & \text{if } i = j \neq (N-1) \\ 0 & \text{otherwise} \end{cases} \tag{8}$$

an $(N-1)$-length column vector

$$\bar{v} = \begin{bmatrix} V_1 & V_2 & \dots & V_{N-2} & V_{N-1} \end{bmatrix}^T \tag{9}$$

and an $(N-1) \times 2$ matrix

$$\mathbf{B} = \begin{cases} 1 & \text{if } i = j = 1 \\ 1 & \text{if } i = (N-1) \text{ and } j = 2 \\ 1 & \text{if } N > 2, i = 2, \text{ and } j = 1 \\ 1 & \text{if } N > 2, i = (N-2), \text{ and } j = 2 \\ 0 & \text{otherwise.} \end{cases} \tag{10}$$

Note that all values of V_0 and V_N have been moved to the right-hand side of (5), as they are considered fixed voltages that

govern the intermediate voltages. By simplifying the left-hand side of (5) into a single matrix and dividing by $(C+S)$, (5) can be reduced to

$$\mathbf{A}\bar{v} = \mathbf{B}\begin{bmatrix} V_0 \\ V_N \end{bmatrix} \tag{11}$$

where the $(N-1)\times(N-1)$ matrix $\mathbf{A}$ is

$$\mathbf{A}(i,j) = \begin{cases} \epsilon & \text{if } i=j\neq(N-1) \\ \zeta & \text{if } i=j=(N-1) \\ -1 & \text{if } i=j\pm 2 \\ 0 & \text{otherwise} \end{cases} \tag{12}$$

and

$$\epsilon = \frac{3C+3S+P}{C+S} \tag{13}$$

$$\zeta = \frac{2C+3S}{C+S}. \tag{14}$$

The LU-decomposition of A is

$$\mathbf{A} = \mathbf{L}\mathbf{U} \tag{15}$$

where

$$\mathbf{L} = \begin{cases} 1 & \text{if } i=j \\ -1/g_{(i-1)/2} & \text{if } i=j+2 \text{ and } i \text{ is odd} \\ -1/g_{(i/2)-1} & \text{if } i=j+2 \text{ and } i \text{ is even} \\ 0 & \text{otherwise} \end{cases} \tag{16}$$

$$\mathbf{U} = \begin{cases} -1 & \text{if } i=j-2 \\ g_{(i+1)/2} & \text{if } i=j\neq(N-1) \text{ and } i \text{ is odd} \\ g_{(i/2)} & \text{if } i=j\neq(N-1) \text{ and } i \text{ is even} \\ h_{(i+1)/2} & \text{if } i=j=(N-1) \text{ and } i \text{ is odd} \\ h_{(i/2)} & \text{if } i=j=(N-1) \text{ and } i \text{ is even} \\ 0 & \text{otherwise} \end{cases} \tag{17}$$

and

$$g_n = \begin{cases} \epsilon & \text{if } n=1 \\ \epsilon - \frac{1}{g_{n-1}} & \text{if } n>1 \end{cases} \tag{18}$$

$$h_n = g_n - \epsilon + \zeta. \tag{19}$$

Solving the recurrence relation in (18) results in the closed formula

$$g_n = \frac{\gamma}{1-(\gamma-\epsilon)^n(-\gamma-\epsilon)^{-n}} - \frac{1}{2}(\gamma-\epsilon) \tag{20}$$

where

$$\gamma = \sqrt{\epsilon^2-4}. \tag{21}$$

Equations (16)–(19) can be proven by substituting them into the right-hand side of (15), substituting (12) into the left-hand side of (15), and verifying equality.

By summing the charges into V_N in both phases of Fig. 3, the output charge to V_N during one complete FQP cycle is found to be

$$\begin{aligned}\Delta q_N = {} & S[(V_{N-1}-V_N)-(0)] + S[(V_{N-2}-V_N)-(0)] \\ & -C[(V_N-V_{N-2})-(V_{N-1})].\end{aligned} \tag{22}$$

This simplifies to

$$\Delta q_N = (C+S)(V_{N-2}+V_{N-1}) - (C+2S)V_N. \tag{23}$$

By replacing the first capacitor in Fig. 3 with a voltage source V_0, it can be seen that (23) applies to $N=1$ by replacing values V_{N-2} and V_{N-1} with V_0. With this, and by applying (11) and (15) to (23) for $N>1$, (23) can be represented for all physical values of N as

$$\Delta q_N = \begin{cases} 2(C+S)V_0 - (C+2S)V_N & \text{if } N=1 \\ (C+S)\left(V_0 + \mathbf{U}^{-1}\mathbf{L}^{-1}\mathbf{B}\begin{bmatrix} V_0 \\ V_N \end{bmatrix}\right) & \\ \quad -(C+2S)V_N & \text{if } N=2 \\ (C+S)w\mathbf{U}^{-1}\mathbf{L}^{-1}\mathbf{B}\begin{bmatrix} V_0 \\ V_N \end{bmatrix} & \\ \quad -(C+2S)V_N & \text{if } N>2 \end{cases} \tag{24}$$

where w is a $1\times(N-1)$ row vector

$$w = \begin{cases} 1 & \text{if } j=(N-1) \text{ or } j=(N-2) \\ 0 & \text{otherwise} \end{cases} \tag{25}$$

and where $\mathbf{L^{-1}}$ and $\mathbf{U^{-1}}$, which are the inverses of (16) and (17), respectively, are

$$\mathbf{L}^{-1} = \begin{cases} 1 & \text{if } i=j \\ \prod_{n=(j+1)/2}^{(i-1)/2} g_n^{-1} & \text{if } i>j \text{ and } i,j \text{ are odd} \\ \prod_{n=j/2}^{(i/2)-1} g_n^{-1} & \text{if } i>j \text{ and } i,j \text{ are even} \\ 0 & \text{otherwise} \end{cases} \tag{26}$$

and $\mathbf{U^{-1}}$ is shown in (27) at the bottom of the next page. Equations (26) and (27) can be proven by multiplying (26) by (16) and by multiplying (27) by (17) and verifying equality to the identity matrix in both cases. Note that if the Capital Pi notation has an upper index less than the lower index, the product is simply 1. This renders the third and fourth cases as $h^{-1}_{(j+1)/2}$ and $h^{-1}_{j/2}$ in the rightmost column of $\mathbf{U}^{-1}$, respectively.

The output voltage for the standard model of an unregulated charge pump, as seen in [8, Fig. 6], is of the form

$$V_N = V_0 \times G - R_{\text{OUT}} \times I_N \tag{28}$$

which can be rearranged and related to (24) as

$$(\Delta q_N)f = I_N = \frac{G}{R_{\text{OUT}}}V_0 - \frac{1}{R_{\text{OUT}}}V_N. \tag{29}$$

For the case of $N = 1$, R_{OUT} and G can be found by inspecting (24) and comparing it with (29). For the case of $N > 1$, R_{OUT} and G can be found by substituting (10), (26), and (27) into (24) and relating the result to (29). The output characteristics are then found to be

$$R_{\text{OUT}} = \begin{cases} \dfrac{1}{f(C+2S)} & \text{if } N = 1 \\ \dfrac{h_1}{f\left[(C+2S)h_1 - (C+S)\right]} & \text{if } N = 2 \\ \dfrac{g_r h_t}{f\left[(C+2S)g_r h_t - (C+S)(g_r+h_t)\right]} & \text{if } N > 2 \end{cases} \tag{30}$$

and

$$G = \begin{cases} \dfrac{2(C+S)}{C+2S} & \text{if } N = 1 \\ \dfrac{(C+S)(h_1+1)}{(C+2S)h_1 - (C+S)} & \text{if } N = 2 \\ \dfrac{(C+S)X\left(\prod_{n=1}^{r-1} g_n^{-1}\right)}{(C+2S)g_r h_t - (C+S)(g_r+h_t)} & \text{if } N > 2 \end{cases} \tag{31}$$

where

$$r = \text{floor}\left(\frac{N-1}{2}\right) \tag{32}$$

$$t = \text{ceil}\left(\frac{N-1}{2}\right) \tag{33}$$

$$X = \begin{cases} g_r + h_t & \text{if } N \text{ is odd} \\ 1 + h_t & \text{if } N \text{ is even.} \end{cases} \tag{34}$$

The product in (31) is replaced with the following closed-form equation:

$$\prod_{n=1}^{r-1} g_n^{-1} = \frac{\gamma(-2)^r(\gamma-\epsilon)^{-r}}{\left(\frac{\epsilon+\gamma}{\epsilon-\gamma}\right)^r - 1}. \tag{35}$$

Therefore, (30) and (31) are completely closed-form formulas to the output characteristics of an FQP. These equations use the values of (19)–(21) and (32)–(35), which are in turn functions of switching and parasitic capacitances through (13) and (14).

C. Observations of Closed-Form Analytic Formula

1) Ideal Output Characteristics: One of the first observations one may make is the limiting case of an ideal FQP. In the ideal circuit where S and P equal 0, the results greatly simplify, since pattern-matching of (18) and (19) shows that

$$g_{n,\,\text{ideal}} = \frac{F_{2n+2}}{F_{2n}} \tag{36}$$

$$h_{n,\,\text{ideal}} = \frac{F_{2n+1}}{F_{2n}} \tag{37}$$

where F_n is the nth element in the Fibonacci sequence

$$F_n = \begin{cases} 1 & \text{if } n = 1 \text{ or } n = 2 \\ F_{n-2} + F_{n-1} & \text{if } n > 2. \end{cases} \tag{38}$$

By substituting (36)–(38) into (30) and (31) when $S = 0$ and applying Cassini's Theorem, the ideal output characteristics reduce to

$$R_{\text{OUT,\,ideal}} = \frac{F_N F_{N+1}}{Cf} \tag{39}$$

$$G_{\text{ideal}} = F_{N+2} \tag{40}$$

which matches the gain results of [3]. Analysis shows that $R_{\text{OUT,\,ideal}} \geq R_{\text{OUT}}$ for all physical values of C, S, and P, which is an analytic explanation of these same experimental observations from [6]. Similarly, $G_{\text{ideal}} \geq G$.

2) Limit of Large N: The limit of the output characteristics as N approaches infinity is also determined. First, by solving the continued fraction of (18), the limit of g_n is found to be

$$\lim_{n\to\infty} g_n = g_\infty = \frac{\epsilon + \sqrt{\epsilon^2 - 4}}{2}. \tag{41}$$

By applying (41) to (30), the limit of R_{OUT} is found to be

$$\lim_{N\to\infty} R_{\text{OUT}} = \frac{1}{f[(1-\Gamma)C + (2-\Gamma)S]}$$
$$\text{where } \Gamma = \frac{2}{\epsilon + \sqrt{\epsilon^2-4}} + \frac{2}{2\zeta - \epsilon + \sqrt{\epsilon^2-4}}. \tag{42}$$

On the other hand, due to the product in (31), G becomes

$$\lim_{N\to\infty} G = 0. \tag{43}$$

This indicates that the load-dependent losses become constant as N increases for a current-load or fall to 0 as N increases for a resistive load. With a resistive load, it is entirely the load-independent losses that cause the output voltage to fall to 0.

3) Effects of P: Since $h_1 = \zeta$, it is seen from (30) and (31) that the output characteristics when $N = 1$ or $N = 2$ are entirely

$$\mathbf{U}^{-1} = \begin{cases} \prod_{n=(i+1)/2}^{(j+1)/2} g_n^{-1} & \text{if } i \leq j < (N-1) \text{ and } i,\ j \text{ are odd} \\ \prod_{n=i/2}^{j/2} g_n^{-1} & \text{if } i \leq j < (N-1) \text{ and } i,\ j \text{ are even} \\ \left(\prod_{n=(i+1)/2}^{(j-1)/2} g_n^{-1}\right) h_{(j+1)/2}^{-1} & \text{if } i \leq j = (N-1) \text{ and } i,\ j \text{ are odd} \\ \left(\prod_{n=i/2}^{(j/2)-1} g_n^{-1}\right) h_{j/2}^{-1} & \text{if } i \leq j = (N-1) \text{ and } i, j \text{ are even} \\ 0 & \text{otherwise.} \end{cases} \tag{27}$$

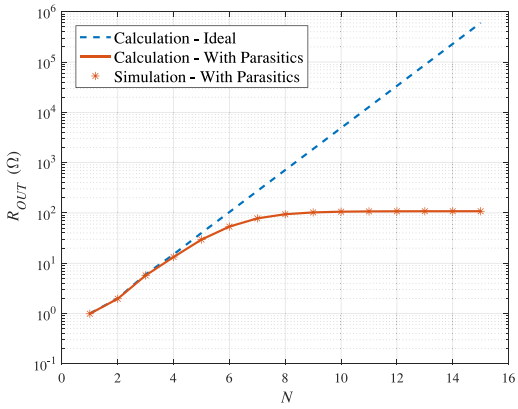

Fig. 4. R_{OUT} over number of stages, N, for calculation (solid line) and simulation (asterisk) of circuit with parasitics described in Section II-D. Well-known ideal calculation (dashed line) plotted as well to illustrate effect of parasitics.

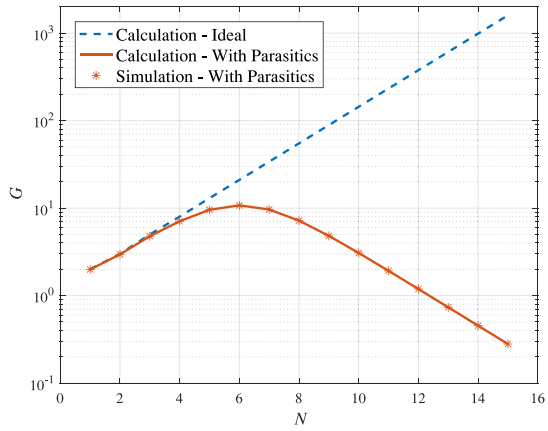

Fig. 5. G over number of stages, N, for calculation (solid line) and simulation (asterisk) of circuit with parasitics described in Section II-D. Well-known ideal calculation (dashed line) plotted as well to illustrate effect of parasitics.

independent of P, which is the sum of the low-side switch and bottom-plate capacitances. Although P affects the open-circuit input conductance and thus the efficiency, it has no effect on the output voltage for $N = 1$ and $N = 2$ in this FQP model. Cabrini *et al.* [3] commented on this observation by stating that the bottom-plate parasitic capacitors draw no charge for $N = 1$ and $N = 2$ but should have more clearly stated that they are charged directly from the input voltage source for the first two bottom-plate parasitic capacitors.

4) Computation: One substantial benefit of the closed-form formula derived here is that the number of computations required is constant for $N > 2$. In other words, the complexity to compute the output characteristics through the formulas presented in this letter is $\mathcal{O}(1)$ over N. This is very different from the common matrix-based approaches of [1], [4]–[6] where the characteristic matrix computations grow linearly with N.

D. Simulation Verification

In addition to the partial verification of (30) and (31) through their degeneration to previously published results, simulations for an example circuit have been performed using LTspice. R_{OUT} and G were simulated for the case of f of 1 MHz, C of 1 μF, S of 5 nF, and P of 10 nF for N between 1 and 15. Simulations calculated R_{OUT} and G by looking at the output voltage 1 s after startup with a 1-V input voltage and a 1-mF output capacitor. The simulations were run unloaded and with a 1-Ω load to calculate both parameters for each value of N. Figs. 4 and 5 illustrate the calculated behaviors discussed in Section II-C of this example circuit when S and P were valued as in the simulation [labeled "Calculation—With Parasitics" as solid lines and calculated through (30) and (31)] and when they were equal to 0 [labeled "Calculation—Ideal" as dashed lines and calculated through (39) and (40)]. Errors between the simulation (labeled "Simulation—With Parasitics" as asterisks) and calculation including parasitics were always less than 0.013%, verifying correct derivations of the output characteristic equations. Any error was likely due to the effects of the transient and computational limits.

III. Conclusion

A fully closed-form analytic formula to the FQP output characteristics including bottom-plate and closed-switch parasitic capacitances have been derived with a complete generalization to N stages. Previous approaches required that large matrices be recomputed for any change in capacitance, frequency, or number of stages to determine the output characteristics of an FQP with parasitics. With the analytic formulas presented in this letter, sweeping over multiple parameters becomes much faster and simpler, both computationally and intuitively. Analytic results have given insight into the behavior at the limits when parasitics fall to 0 and into which losses dominate as N grows. The formulas can be used to more quickly optimize FQP designs with single values of C, a very realistic design choice. The results have also been shown to reduce exactly to the results of special cases from other works and are confirmed with simulation.

References

[1] M. D. Seeman, "A design methodology for switched-capacitor dc-dc converters," Tech. Rep. EECS-2009-78, Univ. California, Berkeley, Berkeley, CA, USA, May 2009.

[2] M. S. Makowski and D. Maksimovic, "Performance limits of switched-capacitor dc-dc converters," in *Proc. Power Electron. Spec. Conf.*, Jun. 1995, vol. 2, pp. 1215–1221.

[3] A. Cabrini, L. Gobbi, and G. Torelli, "Voltage gain analysis of integrated fibonacci-like charge pumps for low power applications," *IEEE Trans. Circuits Syst. II, Exp. Briefs*, vol. 54, no. 11, pp. 929–933, Nov. 2007.

[4] T. Tanzawa, "On two-phase switched-capacitor multipliers with minimum circuit area," *IEEE Trans. Circuits Syst. I, Reg. Papers*, vol. 57, no. 10, pp. 2602–2608, Oct. 2010.

[5] M. D. Seeman and S. R. Sanders, "Analysis and optimization of switched-capacitor dc-dc converters," *IEEE Trans. Power Electron.*, vol. 23, no. 2, pp. 841–851, Mar. 2008.

[6] E. Ferro, V. M. Brea, P. Lopez, and D. Cabello, "Dynamic model of switched-capacitor dc-dc converters in the slow-switching limit including charge reusing," *IEEE Trans. Power Electron.*, vol. 32, no. 7, pp. 5293–5311, Jul. 2017.

[7] W. Ki, Y. Lu, F. Su, and C. Tsui, "Design and analysis of on-chip charge pumps for micro-power energy harvesting applications," in *Proc. IEEE/IFIP 19th Int. Conf. VLSI Syst.-on-Chip*, Oct. 2011, pp. 374–379.

[8] A. Cabrini, L. Gobbi, and G. Torelli, "A theoretical charge transfer scheme for efficiency optimization of integrated charge pumps," in *Proc. 21st IEEE Int. Conf. Electron., Circuits Syst.*, Dec. 2014, pp. 303–306.